HHS Public Access

Author manuscript

Drug Deliv Transl Res. Author manuscript; available in PMC 2019 August 01.

Published in final edited form as:

Drug Deliv Transl Res. 2018 August ; 8(4): 954–963. doi:10.1007/s13346-017-0412-5.

Optimizing endothelial cell functionalization for cell therapy of vascular proliferative disease using a direct contact co-culture system

Mark R. Battig[1], **Ilia Fishbein**[1], **Robert J. Levy**[1], **Ivan S. Alferiev**[1], **David Guerrero**[1], and **Michael Chorny**[1]

[1]Division of Cardiology, The Children's Hospital of Philadelphia, and Department of Pediatrics, Perelman School of Medicine, Philadelphia, PA 19104, USA

Abstract

Increased susceptibility to thrombosis, neoatherosclerosis, and restenosis due to incomplete regrowth of the protective endothelial layer remains a critical limitation of the interventional strategies currently used clinically to relieve atherosclerotic obstruction. Rapid recovery of endothelium holds promise for both preventing the thrombotic events and reducing post-angioplasty restenosis, providing the rationale for developing cell delivery strategies for accelerating arterial reendothelialization. The successful translation of experimental cell therapies into clinically viable treatment modalities for restoring vascular endothelium critically depends on identifying strategies for enhancing the functionality of endothelial cells (EC) derived from high cardiovascular risk patients, the target group for the majority of angioplasty procedures. Enhancing EC-associated nitric oxide (NO) synthesis by inducing overexpression of NO synthase (NOS) has shown promise as a way of increasing paracrine activity and restoring function of EC. In the present study, we developed a direct contact co-culture approach compatible with highly labile effectors, such as NO, and applied it for determining the effect of EC functionalization via NOS gene transfer on the growth of co-cultured arterial smooth muscle cells (A10 cell line) exhibiting the defining characteristics of neointimal cells. Bovine aortic endothelial cells magnetically transduced with inducible NOS-encoding adenovirus (Ad) formulated in zinc oleate-based magnetic nanoparticles (MNP[$_{iNOS}$Ad]) strongly suppressed growth of proliferating A10 and attenuated the stimulatory effect of a potent mitogen, platelet-derived growth factor (PDGF-BB), whereas EC functionalization with free $_{iNOS}$Ad or MNP formulated with a different isoform of the enzyme, endothelial NOS, was associated with lower levels of NO synthesis and less pronounced antiproliferative activity toward co-cultured A10 cells. These results show feasibility of applying magnetically facilitated gene transfer to potentiate therapeutically relevant effects of EC for targeted cell therapy of restenosis. The direct contact co-culture methodology provides a sensitive and reliable tool with potential utility for a variety of biomedical applications.

Correspondence to: Michael Chorny.

Compliance with ethical standards

Competing interests The authors declare that they have no conflict of interest.

Keywords

Direct contact co-culture system; Stent angioplasty; Nitric oxide; Endothelial cell; Smooth muscle cell; Magnetic nanoparticle

Introduction

Injury-triggered arterial renarrowing (restenosis) remains a major limitation of stent angioplasty clinically used to relieve obstruction in coronary and peripheral vasculature. Drug eluting stents (DES) designed to provide site-specific delivery of antiproliferative agents have significantly reduced the incidence of coronary artery restenosis [1]; however, their inhibitory effect on regeneration of functional endothelium has been shown to result in increased rates of subacute and late thrombosis [2, 3], in-stent neoatherosclerosis [4–6], as well as late catch-up in neointimal response [7, 8], all contributing to eventual stent failure [7–9]. In the DES era, current rates of in-stent restenosis (ISR) in patients with complex lesions still exceed 10% [9], with DES-ISR presenting a markedly greater therapeutic challenge [10–12] as evidenced by clinical recurrences about twice as frequent in comparison to those seen with bare metal stents [13].

Restoration of functionally and structurally intact endothelium plays an important role in the arterial healing after injury [14, 15]. In addition to forming an anatomical barrier separating the blood stream from the vessel wall and preventing platelet deposition and inflammatory cell invasion, endothelial cells (EC) exert paracrine effects inhibiting dedifferentiation and inducing mitogenic quiescence of vascular smooth muscle cells [15], all key to mitigating the progression of vessel renarrowing [16, 17]. The promise of reendothelialization-oriented approaches capable of favorably modulating the healing process and reducing injury-triggered intimal hyperplasia without provoking the serious complications associated with currently used DES has prompted exploring EC delivery as an alternative experimental treatment modality for preventing arterial restenosis [18, 19]. However, low efficiency of cell homing and engraftment at the injury site and the generally reduced function of EC derived from high cardiovascular risk patients [20–22], the target group for the majority of stenting procedures, were shown to be the main factors limiting the effectiveness and potential clinical utility of autologous EC in the context of restenosis therapy [19, 23, 24]. Thus, despite the long recognized therapeutic potential of strategies aimed at promoting early endothelium recovery [25], their realization in clinical practice as a viable solution for preventing ISR and late stent failure continues to pose a need for conceptually novel approaches both providing significantly improved cell homing rates and restoring cell functionality.

Magnetically guided cell delivery is emerging as a promising experimental strategy for accelerating endothelium recovery in stented blood vessels [26–30]. Our group has recently reported rapid and stable EC homing and expansion in stented arteries [31] achievable with two-source magnetic guidance, previously shown to be effective for site-specific vascular delivery of small-molecule drugs and gene vectors [32, 33]. Unlike other approaches using a single magnetic field source, the two-source strategy taking advantage of highly localized

field gradients created in proximity of a reversibly magnetizable stent during exposure to a uniform field of a clinically applicable strength can be applied for targeting non-superficial sites [34–36] and is scalable to large blood vessels [37]. This approach can be readily extended to cell delivery applications by endowing therapeutic cells with magnetic guidance capacity. We and others have shown that magnetically facilitated internalization of magnetite-loaded biodegradable nanoparticles (MNP) is an effective strategy for providing EC with magnetic responsiveness [26, 31, 38]. Intriguingly, the step of loading cells with MNP can also be exploited to concomitantly introduce genetic modifications and restore therapeutically relevant autocrine and paracrine activity of EC [30]. In the context of cell therapy for preventing arterial restenosis, the nitric oxide (NO) synthase/NO effector system stands out as particularly promising due to advantages of NO as a potent and pleiotropic small-molecule effector acting on different cell populations and multiple pathways involved in the restenosis pathophysiology [39]. The therapeutic potential of increasing NO production levels and enhancing the paracrine activity of EC via genetic modification is supported by several studies showing markedly enhanced antirestenotic effect of NO synthase-overexpressing cells in experimental settings [30, 40]. Based on experimental evidence, the ability of NO to inhibit proliferation of arterial smooth muscle cells (SMC) by both cGMP-dependent and cGMP-independent mechanisms is one of the primary factors contributing to the greater potency of EC functionalized with the NO synthase/NO effector system [41, 42], suggesting that optimization of the EC functionalization strategy for clinical translation should address SMC growth inhibition and elucidate its dependence on EC loading protocol and MNP formulation variables. However, directly measuring the effect of EC-derived NO on SMC growth is challenging since NO has a short lifetime and diffuses short distances from its site of production [43, 44], which makes the use of standard cell co-culture techniques impractical [41].

In the present study, we introduced a new direct contact co-culture system and applied it for measuring the effect of EC functionalized with MNP to overexpress inducible NO synthase (iNOS) on the proliferation rates of rat aortic SMC (A10) exhibiting the defining characteristics of neointimal smooth muscle cells [45]. We have previously reported on the design and properties of MNP formulations facilitating the uptake and intracellular processing of adenoviral vectors (Ad) and enabling effective magnetically driven gene transfer concomitantly with imparting magnetic responsiveness to EC [33, 38, 46]. Here, using a new quantitative assay that addresses the challenges posed by the poor stability of the small-molecule effector, we evaluated MNP[$_{iNOS}$Ad]-driven modulation of the enzymatic NO synthesis by EC as a way of regulating the proliferation rates of vascular SMC. This analytical method provides a reliable tool for estimating in vitro the paracrine component contributing to the overall antirestenotic activity of functionalized EC and for optimizing these cells as a biotherapeutic agent for treating vascular proliferative conditions.

Materials and methods

MNP formulation and characterization

Type 5 first-generation $_{iNOS}$Ad and $_{eNOS}$Ad under the control of the CMV promoter used in this study were provided by the Gene Transfer Vector Core of the University of Iowa (Iowa

City, IA, USA). MNP[Ad] were formulated with zinc oleate as the matrix-forming material using a controlled precipitation process as reported previously [33]. In brief, iron oxide was first produced by adding 2.5 ml of an ethanolic solution containing 170 mg ferric chloride hexahydrate (Sigma-Aldrich, St. Louis, MO, USA) and 62.5 mg of ferrous chloride tetrahydrate (Acros Organics/Fisher Scientific USA, Pittsburgh, PA, USA) to 5 ml of an aqueous sodium hydroxide solution (5 N), followed by incubation at 90 °C for 1 min. The obtained precipitate was resuspended in 5 ml of an aqueous solution containing 225 mg of sodium oleate (Sigma-Aldrich) and converted to colloidal dispersion of oleate-stabilized magnetite by two 5-min heating/sonication cycles (90 °C). The dispersion was passed sequentially through a 1.0-μm glass fiber prefilter (Millipore Billerica, MA, USA) and a sterile 0.45-μm glass/acetate filter (GE Water & Process Technologies, Trevose, PA, USA) into a presterilized vial. In the next step, 200 μl of an aqueous sterile-filtered solution of Pluronic F-127 (10% *w*/*v*) and 100 μl containing 10^{11} Ad particles diluted in deionized water were added to 0.75 ml of the magnetite dispersion. Aqueous zinc chloride (0.75 ml of a 0.1 M solution) was added dropwise to form zinc oleate-based MNP loaded with Ad. The particles were placed on an orbital shaker for 15 min at 4 °C, then washed by two magnetic decantation/resuspension cycles on ice and reconstituted in an ice-cold solution of Pluronic F-127 and glucose (1 and 5% *w*/*v*, respectively). After adjusting the volume to 0.75 ml, MNP[Ad] were frozen overnight at −80 °C, lyophilized over 24 h, stored at −80 °C, and reconstituted in deionized water (Barnstead Nanopure; Thermo Scientific, Dubuque, IA, USA) before use. Blank (Ad-free) MNP were obtained as above with the Ad addition step omitted. Particle size measurements were performed by dynamic light scattering. Hysteresis loops of MNP formulations were obtained using an alternating gradient magnetometer (Princeton Measurements Corp., Princeton, NJ, USA). Magnetite content was determined spectrophotometrically against a suitable calibration curve (λ = 360 nm) in MNP samples dissolved in hydrochloric acid (5 N) by heating to 60 °C for 20 min.

EC functionalization with MNP[Ad] and co-culture studies

For MNP[Ad] functionalization, bovine aortic endothelial cells (BAEC) were seeded at 60% of confluence on 96-well plates. On the next day, the cells were treated for 15 min with MNP[Ad] or free Ad diluted in DMEM containing 10% FBS with/without positioning the plates on a 96-well magnetic separator with an average field gradient of 32.5 T/m (LifeSep 96F; Dexter Magnetic Technologies, Elk Grove Village, IL, USA), then washed twice and incubated with fresh FBS-supplemented DMEM. Untreated BAEC were used as a control. The cells were left overnight under 10% FBS in DMEM before adding A10 stably expressing GFP at 2×10^3 cells per well in DMEM containing 2% FBS and supplemented with 20 ng/ml PDGF-BB. NO production was determined by measuring nitrite as its stable metabolite in cell culture medium using the Griess assay [47]. Resazurin (Alamar Blue) cell viability assay [48] was used to determine viability of MNP-functionalized BAEC, and for validating direct GFP fluorimetric analysis as a cell growth assay for $_{GFP}$A10. In co-culture experiments, the expansion of $_{GFP}$A10 was monitored by fluorescent microscopy using standard fluorescein wavelength settings and determined quantitatively by fluorimetry ($\lambda_{ex}/\lambda_{em}$ = 485 nm/535 nm).

Results are reported as mean ± SD unless stated otherwise. Cell proliferation rates were compared using the single-factor ANOVA. Differences were termed significant at $p < 0.05$.

Results

Zinc oleate-based MNP[$_{iNOS}$Ad] with an average size of 280 ± 10 nm (polydispersity index ≤0.06) and a magnetite loading of 33% (*w*/w) were obtained using a previously reported controlled precipitation approach [33]. This is a solvent-free process carried out under mild conditions, where two aqueous phases containing water-soluble oleate and divalent metal salts are combined in the presence of superparamagnetic nanocrystalline iron oxide, a surfactant and a therapeutic cargo, such as Ad particles, to form colloidally stable MNP. In this process, biocompatible polymers of the polyalkylene glycol family, such as Pluronic F-127 employed here as a surfactant, are essential for both stabilizing and controlling the size of MNP, as well as for preventing destabilization and cargo activity loss during the lyophilization step. The inclusion of magnetite embedded in the particle matrix endows these oleate-based MNP with high magnetic susceptibility (magnetic moments of 28 and 18 emu/g at 1.0 and 0.1 T, respectively) and, in accordance with the superparamagnetic properties of the iron oxide configured in small-sized (≤20 nm) crystallites, the magnetic remanence of the composite particles is negligible (≤1.5% of the saturation magnetization value).

In our previous studies, zinc oleate-based MNP impregnated with Ad and applied to cells with exposure to a high-gradient magnetic field led to high expression levels of reporter proteins or iNOS markedly exceeding those achievable with free Ad [33], demonstrating that magnetically driven gene transfer with MNP[Ad] may offer a viable and effective strategy for functionalizing EC. To further examine the therapeutically relevant effects of magnetically facilitated NO synthase gene delivery and the resultant enhancement in EC-associated enzymatic NO synthesis, the present study focused on the development and characterization of a direct contact co-culture system in combination with a cell type-specific proliferation assay (schematically shown in Fig. 1a). We chose to use a clone of SMC derived from the thoracic aorta of embryonic rats and lentivirally transduced to stably express the green fluorescent protein (GFP) reporter for EC/SMC co-culture experiments due to convenient fluorescent microscopy analysis (Fig. 1b–d) and selective and quantitative fluorimetric determination in the presence of other cells. Notably, these poorly differentiated vascular SMC (A10 clonal cell line, [49]) have previously been shown to closely reproduce key features of neointimal cells [45]. The majority of $_{GFP}$A10 cells seeded on top of a monolayer of bovine aortic endothelial cells (BAEC) showed stable attachment and spreading, with the proportion and morphology of the spreading $_{GFP}$A10 cells unaltered by EC pretreatment with zinc oleate-based MNP (Fig. 1c vs. b). Specificity of the green fluorescence associated with GFP-expressing A10 was confirmed in an experiment demonstrating feasibility of using the green channel for observing and measuring growth of SMC, while simultaneously monitoring the expression of a model transgene by EC, with the red fluorescent protein (RFP) employed as a second marker quantifiable using a different set of excitation/emission wavelengths (Fig. 1d).

Experimental conditions optimal for selectively stimulating co-cultured SMC were identified by examining growth kinetics of $_{GFP}$A10 in the presence of a potent and cell type-specific mitogen, platelet-derived growth factor (PDGF-BB) [50] added to low serum culture medium (DMEM with 2% FBS). $_{GFP}$A10 cells initially seeded at 10% confluence were exposed to increasing concentrations of PDGF-BB (2–40 ng/ml). Under high PDGF-BB conditions, $_{GFP}$A10 rapidly expanded reaching a near-confluent state by day 7, whereas markedly lower rates of expansion were observed for cells exposed to decreasing concentrations of the mitogen (Fig. 2b, d vs. a, c). These findings were confirmed quantitatively by measuring $_{GFP}$A10 growth kinetics using living cell fluorimetry ($\lambda_{ex}/\lambda_{em}$ = 485 nm/535 nm). Fluorimetric measurements revealed a dose-dependent response of proliferating $_{GFP}$A10 to the growth factor added to the culture medium, with cell numbers plateauing at PDGF-BB concentrations exceeding 20 ng/ml (Fig. 2e). The results of the direct GFP fluorimetric measurements were in good agreement with those obtained using an established resazurin (Alamar Blue) cell viability assay [48] (Fig. 2f), suggesting that cell-associated fluorescence can be used reliably for quantifying proliferating SMC. The presence of PDGF-BB had no growth stimulatory effect on BAEC as expected based on the limited to no PDGF receptor expression reported for EC [51]. Based on these results, culture conditions using a low-serum growth medium supplemented with PDGF-BB (20 ng/ml) were found to be optimal for studying the expansion rates of SMC seeded on an EC monolayer, while the cell type-selective proliferation assay based on measuring GFP constitutively expressed by $_{GFP}$A10 cells and quantifiable specifically, without interference from co-cultured EC, provides a simple analytical tool for determining the modulating effects of MNP-functionalized EC on SMC growth.

In a co-culture experiment, the effect of EC functionalization with MNP[$_{iNOS}$Ad] on the growth rate of proliferating $_{GFP}$A10 was compared to those of free $_{iNOS}$Ad or blank MNP formulated without the virus (Fig. 3). On days 3 and 7, a strong growth inhibition of $_{GFP}$A10 was observed in co-culture with BAEC pretreated magnetically with MNP[$_{iNOS}$Ad] in comparison with untreated BAEC used as a reference (Fig. 3d vs. a and h vs. e). Whereas the number of $_{GFP}$A10 grown with MNP[$_{iNOS}$Ad]-functionalized BAEC increased only marginally between days 3 and 7, $_{GFP}$A10 co-cultured with BAEC untreated or treated with blank MNP or free Ad expanded significantly over the same time period. Interestingly, the growth patterns of $_{GFP}$A10 also appeared to be dependent on the EC functionalization strategy: the majority of $_{GFP}$A10 co-cultured with MNP[$_{iNOS}$Ad]-treated BAEC were present as single cells at both days 3 and 7, with no signs of lining up in parallel arrays (Fig. 3d, h), unlike clustered and notably more aligned $_{GFP}$A10 growing on BAEC non-functionalized or treated with blank MNP or free vector controls.

Quantitative analysis of the A10 response to BAEC functionalization revealed a strong, direct correlation with the MNP[$_{iNOS}$Ad] dose that paralleled the MNP dose-dependent synthesis of NO by genetically modified BAEC (Fig. 4). The amounts of NO synthesized by MNP[$_{iNOS}$Ad]-transduced BAEC were found to be in the 20–80 μM range 3 days after treatment (Fig. 4a), and doubled by day 7. With the result seen with the lowest tested dose of MNP corresponding to 20×10^6 viral particles (v.p.) being the only exception, $_{GFP}$A10 growth inhibition also nearly doubled from day 3 to 7, reaching 44 ± 1 and 97 ± 1% at doses equivalent to 25×10^6 and 50×10^6 v.p., respectively. Interestingly, Ad-free blank MNP,

showing no detectable stimulation of NO synthesis by BAEC, had an opposite effect on the growth of co-cultured $_{GFP}$A10 markedly promoting their expansion by day 7 based on the results of fluorimetric analysis (Fig. 4a, c).

It is noteworthy that BAEC treatment with free $_{iNOS}$Ad or with MNP[$_{iNOS}$Ad] applied under non-magnetic conditions had a readily detectable growth inhibitory effect on co-cultured $_{GFP}$A10 (Fig. 5) despite a limited enhancement of EC-associated NO production activity in comparison to magnetically enhanced gene delivery (Figs. 5a vs. 4a). In agreement with the strengths of the respective stimulatory effects on NO synthesis, a stronger $_{GFP}$A10 growth inhibition (up to 60%) was generally seen with MNP[$_{iNOS}$Ad] applied to BAEC in the absence of magnetic exposure than with free $_{iNOS}$Ad that uniformly remained below 40% within the tested dose range. However, the dose dependence of this effect was substantially less pronounced than with magnetically driven MNP[$_{iNOS}$Ad]-mediated transduction, and the relative increase in $_{GFP}$A10 growth inhibition between days 3 and 7 was also smaller in comparison to magnetically facilitated iNOS gene transfer (Fig. 5b, c).

EC functionalization with endothelial NO synthase (eNOS) was examined in comparison to iNOS transduction. Notably, while BAEC transduced with free eNOS had little effect on $_{GFP}$A10 growth, magnetically enhanced eNOS gene transfer using MNP resulted in a detectable $_{GFP}$A10 growth inhibition 7 days post treatment peaking at 28 ± 1% at a dose corresponding to 45×10^6 v.p. However, the $_{GFP}$A10 growth inhibitory effect achievable with MNP[$_{eNOS}$Ad]-mediated BAEC functionalization was notably weaker in comparison to that of MNP[$_{iNOS}$Ad] at comparable doses (Fig. 6).

Discussion

Treating obstructive vascular disease effectively without provoking serious complications remains an elusive goal: recent studies point to the emergence of particularly challenging varieties of restenosis [7, 9] and susceptibility to thrombosis that may remain unchanged with no decline in event rates over 10 years in patients implanted with DES releasing antimitotic drugs [52]. New therapeutic strategies aiming to accomplish rapid regrowth of vascular endothelium and restoring its vasoprotective effect through site-specific delivery of functionalized EC have potential to both prevent the thrombotic events and limit post-angioplasty restenosis [16, 17, 53], thereby addressing the limitations of existing DES.

EC functionalization with MNP to provide cells with capacity for magnetic guidance and stent-targeted delivery while simultaneously restoring their ability to exert therapeutically relevant paracrine effects mediated by enzymatically synthesized NO is an experimental approach that, if successfully scaled up from preclinical studies to testing in cardiovascular disease patients, may pave the way to achieving magnetically accelerated, rapid endothelium restoration with significant improvement of vascular function [30]. However, the translation of this approach critically depends on learning about key variables controlling EC actuation by the MNP-mediated genetic modification process and reliably measuring its effect on other types of vascular cells contributing to arterial restenosis. Direct contact co-culture of EC with quiescent arterial SMC has previously been developed and applied successfully to learn about interactions between the two cell types under conditions modeling a healthy

vessel wall [54, 55]. In the present study, our goals were to (1) extend the utility of the direct contact co-culture approach to examining the paracrine effects of EC on proliferating SMC, and (2) apply this method for observing and quantitatively measuring the effect of modulating NO synthetic activity of EC on the growth of de-differentiated SMC phenotypically resembling neointimal cells. As part of feasibility studies, we demonstrated that cloned $_{GFP}$A10 cells maintain their proliferative phenotype and retain responsiveness to a cell type-specific mitogen, PDGF-BB strongly contributing to intimal hyperplasia in vivo [50, 56]. We also showed that stable GFP expression provides a sensitive tool for monitoring continuously and selectively the morphology and number of co-cultured SMC seeded on top of an EC monolayer.

The direct contact co-culture methodology offers a number of advantages, which are worth mentioning. It enables simultaneous analysis of the effects of multiple variables in the cell functionalization process and/or MNP design. The assay allows selectively and quantitatively determining cells of a particular type in the presence of “donor” cells producing the effector. The co-culture setting employed in this approach models the direct contact experienced by cells in vivo, within the environment of the vessel wall. An important advantage of this direct contact co-culture methodology is that it is applicable to studying cell interactions driven by short-lived effectors, such as NO that rapidly decomposes after its synthesis invalidating results obtained using standard co-culture techniques [41]. The assay is also non-destructive, enabling kinetic measurements with several time points, in combination with concomitant analysis of the effector levels in the medium.

We previously showed that magnetically facilitated gene transfer to EC using zinc oleate-based MNP impregnated with $_{iNOS}$Ad can achieve a lasting increase in EC-associated NO synthesis without causing cell toxicity [33]. The results of our present co-culture studies show that iNOS overexpression by MNP-functionalized EC up to 80 μM over 3 days potently inhibits growth of $_{GFP}$A10, with the effect markedly increasing in magnitude from day 3 to day 7 and reaching nearly complete growth inhibition at the higher MNP doses by day 7. Interestingly, whereas substantially lower NO production levels were observed in BAEC treated either with free $_{iNOS}$Ad or MNP[$_{iNOS}$Ad] applied to cells without the magnetic exposure, these moderate increases in NO synthetic activity were sufficient for a readily detectable reduction in proliferation rates of co-cultured A10, although generally smaller and with a notably less pronounced dose dependence than seen with magnetically applied MNP[$_{iNOS}$Ad]. This result suggests distinct mechanisms that govern the growth inhibitory effect on SMC at different levels of EC genetic modification with iNOS. Previous studies have shown that the direct action of NO on SMC can involve both cGMP-dependent and independent mechanisms, with primarily cytostatic effects seen within a lower concentration range [42]. Furthermore, NO is not the only product of NO synthase that may affect SMC proliferation. Both *N*-hydroxyarginine, the principal intermediate in the NOS-catalyzed conversion of arginine to NO, and the reactive oxygen and nitrogen species whose production by the enzyme increases in conditions of cofactor deficiency are also potent regulators of SMC viability and growth [42, 57]. Our findings indicate that up to a certain threshold, likely below 1 μM, a cytostatic effect showing limited dependence on NO production is operational, but a different mechanism with a strong NO amount-effect correlation may become dominant when NO concentrations exceed 10 μM. These

mechanisms may involve two or more complementary or alternate pathways and different effector molecules that may act on their distinct cellular targets, depending on the expression levels of the enzyme and the ratio between its coupled and uncoupled states controlled by cofactor availability. Remarkably, Ad-free MNP having no detectable effect on EC-associated NO production led to a dose-dependent increase in $_{GFP}$A10 proliferation. This effect unrelated to the MNP cargo may be caused by the particle-forming components, such as oleate previously shown to enhance SMC proliferation via the phosphatidylinositol 3-kinase/Akt signaling pathway [58]. However, in accordance with our observations supporting the hypothesis that a moderate increase in EC-associated NO production can already have an effect on PDGF-BB-driven proliferation of intimal SMC, a measurable reduction in proliferation of $_{GFP}$A10 was found in co-culture with EC treated with MNP[Ad] to induce overexpression of endothelial NOS, an enzyme isoform that in contrast to iNOS synthesizes comparatively small amounts of NO in a tightly regulated manner [59].

While this study focuses on evaluating and optimizing EC functionalization based on its ability to reduce proliferation of vascular SMC—a single component among several factors contributing together to the complex pathophysiology of re-stenosis—the methodology and the experimental results may have broad therapeutic implications for effectively treating proliferative vascular diseases. NO is an endogenous effector molecule exerting a diverse range of therapeutically relevant effects which, in addition to maintaining quiescence of vascular SMC, include stimulating endothelium growth [60], inhibiting platelet aggregation and adhesion to vascular endothelium [61, 62], preventing migration of monocytes and neutrophils into the vascular wall [63]. The high diffusivity and the ability to rapidly cross cell membranes make NO a highly efficient mediator. Because of its unique chemical properties and the paracrine mode of action, it has been hypothesized that even a small number of cells overexpressing iNOS may be sufficient to exert a significant antirestenotic effect [64], making integration of the NO synthase/NO effector system in EC functionalized for stent-targeted delivery a promising approach for enhancing cell therapy as a new modality for preventing arterial restenosis.

Notably, while the direct contact co-culture approach evaluated in this study was specifically designed to address the problem posed by rapid inactivation of unstable mediators, such as NO, this assay is also applicable to a variety of molecules from other chemical and pharmacological families capable of enhancing SMC growth suppression by functionalized EC. As an example, an adipocyte-specific secretory protein, adiponectin, has been shown to sequester PDGF-BB, in turn preventing its binding to the receptor, attenuating DNA synthesis, and suppressing PDGF-driven cell proliferation [65]. Thus, adiponectin gene transfer may also be considered as a way of functionalizing EC to achieve vascular SMC growth inhibition by a mechanism distinct from that of the NOS/NO effector system, i.e., by scavenging the mitogen and blocking PDGF-dependent signaling cascades [66]. The development and optimization of this or similar approaches employing secreted proteins as mediators of the antiproliferative action of EC on SMC can also be facilitated by using the direct contact co-culture system introduced in the present work.

Conclusions

The use of gene vectors and small-molecule agents for modulating function of therapeutic cells is expected to play an important role in the design and clinical translation of cell delivery strategies for treating vascular diseases. Sensitive and reliable tools for examining the effectiveness of cell functionalization are needed for identifying promising strategies and optimizing their performance during the preclinical evaluation stage. A direct contact co-culture system reported here was applied for studying the effects of EC functionalized with MNP[Ad] to enhance their NO synthetic activity on mitogen-stimulated proliferative vascular SMC. Our experimental data obtained using this approach show effectiveness of magnetically facilitated gene transfer as a way of functionalizing EC, but also point to the complexity of the paracrine effects mediated by NOS-overexpressing EC underlying distinct patterns of the SMC growth inhibition observed at varying activity levels or with the two different isoforms of the enzyme. In the context of optimizing cell therapy for treating restenosis, the in vitro assay employing cell type-specific culture conditions and selective fluorimetric analysis of proliferating SMC provides a valuable methodology that can be used to inform the development of more efficient cell functionalization strategies. With appropriate modifications, the utility of this direct contact co-culture approach, both as a tool for studying interactions between different cell types and as a practical means for optimizing experimental cell therapies, can be extended to a diverse range of biomedical applications.

Acknowledgments

This research was supported by US National Heart, Lung, and Blood Institute grants T32-HL007915 (MRB), R01-HL111118, and R21-HL131016 (MC); a grant from The W.W. Smith Charitable Trust; and The Children’s Hospital of Philadelphia Research Funds including the William J. Rashkind Endowment, Erin’s Fund, and The Kibel Foundation (RJL).

References

1. Coolong A, Kuntz RE. Understanding the drug-eluting stent trials. Am J Cardiol. 2007; 100(5A): 17K–24K.
2. Guagliumi G, Sirbu V, Musumeci G, Gerber R, Biondi-Zoccai G, Ikejima H, et al. Examination of the in vivo mechanisms of late drug-eluting stent thrombosis: findings from optical coherence tomography and intravascular ultrasound imaging. JACC Cardiovasc Interv. 2012; 5(1):12–20. [PubMed: 22230145]
3. Iakovou I, Schmidt T, Bonizzoni E, Ge L, Sangiorgi GM, Stankovic G, et al. Incidence, predictors, and outcome of thrombosis after successful implantation of drug-eluting stents. JAMA. 2005; 293(17):2126–30. [PubMed: 15870416]
4. Nakazawa G, Finn AV, Virmani R. Vascular pathology of drug-eluting stents. Herz. 2007; 32(4): 274–80. [PubMed: 17607533]
5. Nakazawa G, Otsuka F, Nakano M, Vorpahl M, Yazdani SK, Ladich E, et al. The pathology of neoatherosclerosis in human coronary implants bare-metal and drug-eluting stents. J Am Coll Cardiol. 2011; 57(11):1314–22. [PubMed: 21376502]
6. Otsuka F, Finn AV, Yazdani SK, Nakano M, Kolodgie FD, Virmani R. The importance of the endothelium in atherothrombosis and coronary stenting. Nat Rev Cardiol. 2012; 9(8):439–53. [PubMed: 22614618]
7. Park SJ, Kang SJ, Virmani R, Nakano M, Ueda Y. In-stent neoatherosclerosis: a final common pathway of late stent failure. J Am Coll Cardiol. 2012; 59(23):2051–7. [PubMed: 22651862]
8. Räber L, Serruys PW. Late vascular response following drug-eluting stent implantation. JACC Cardiovasc Interv. 2011; 4(10):1075–8. [PubMed: 22017931]

9. Theodoropoulos K, Mennuni MG, Dangas GD, Meelu OA, Bansilal S, Baber U, et al. Resistant in-stent restenosis in the drug eluting stent era. Catheter Cardiovasc Interv. 2016; 88(5):777–85. [PubMed: 27184223]
10. Alfonso F. Treatment of drug-eluting stent restenosis the new pilgrimage: quo vadis? J Am Coll Cardiol. 2010; 55(24):2717–20. [PubMed: 20538164]
11. Dangas GD, Claessen BE, Caixeta A, Sanidas EA, Mintz GS, Mehran R. In-stent restenosis in the drug-eluting stent era. J Am Coll Cardiol. 2010; 56(23):1897–907. [PubMed: 21109112]
12. Aminian A, Kabir T, Eeckhout E. Treatment of drug-eluting stent restenosis: an emerging challenge. Catheter Cardiovasc Interv. 2008; 74(1):108–16.
13. Steinberg DH, Gaglia MA Jr, Pinto Slottow TL, Roy P, Bonello L, De Labriolle A, et al. Outcome differences with the use of drug-eluting stents for the treatment of in-stent restenosis of bare-metal stents versus drug-eluting stents. Am J Cardiol. 2009; 103(4):491–5. [PubMed: 19195508]
14. Versari D, Lerman LO, Lerman A. The importance of reendothelialization after arterial injury. Curr Pharm Des. 2007; 13(17):1811–24. [PubMed: 17584110]
15. Kipshidze N, Dangas G, Tsapenko M, Moses J, Leon MB, Kutryk M, et al. Role of the endothelium in modulating neointimal formation: vasculoprotective approaches to attenuate restenosis after percutaneous coronary interventions. J Am Coll Cardiol. 2004; 44(4):733–9. [PubMed: 15312851]
16. Douglas G, Van Kampen E, Hale AB, McNeill E, Patel J, Crabtree MJ, et al. Endothelial cell repopulation after stenting determines in-stent neointima formation: effects of bare-metal vs. drug-eluting stents and genetic endothelial cell modification. Eur Heart J. 2012; 34(43):3378–88. [PubMed: 23008511]
17. Fuchs AT, Kuehnl A, Pelisek J, Rolland PH, Mekkaoui C, Netz H, et al. Inhibition of restenosis formation without compromising reendothelialization as a potential solution to thrombosis following angioplasty? Endothelium. 2008; 15(1):85–92. [PubMed: 18568948]
18. Lemos PA. To heal without renarrowing: is it possible to make it real? Catheter Cardiovasc Interv. 2007; 70(5):661. [PubMed: 17960634]
19. Leopold JA. Neoatherosclerosis: another consequence of endothelial dysfunction? Circ Cardiovasc Interv. 2014; 7(5):635–7. [PubMed: 25336601]
20. Cai H, Harrison DG. Endothelial dysfunction in cardiovascular diseases: the role of oxidant stress. Circ Res. 2000; 87(10):840–4. [PubMed: 11073878]
21. Bauersachs J, Thum T. Endothelial progenitor cell dysfunction: mechanisms and therapeutic approaches. Eur J Clin Investig. 2007; 37(8):603–6. [PubMed: 17635570]
22. Thum T, Fraccarollo D, Schultheiss M, Froese S, Galuppo P, Widder JD, et al. Endothelial nitric oxide synthase uncoupling impairs endothelial progenitor cell mobilization and function in diabetes. Diabetes. 2007; 56(3):666–74. [PubMed: 17327434]
23. van Beusekom HM, Serruys PW. Drug-eluting stent endothelium: presence or dysfunction. JACC Cardiovasc Interv. 2010; 3(1):76–7. [PubMed: 20129573]
24. van Beusekom HM, Schoemaker R, Roks AJ, Zijlstra F, van der Giessen WJ. Coronary stent healing, endothelialisation and the role of co-medication. Neth Heart J. 2007; 15(11):395–6. [PubMed: 18612390]
25. Parikh SA, Edelman ER. Endothelial cell delivery for cardiovascular therapy. Adv Drug Deliv Rev. 2000; 42(1–2):139–61. [PubMed: 10942819]
26. Polyak B, Medved M, Lazareva N, Steele L, Patel T, Rai A, Rotenberg MY, Wasko K, Kohut AR, Sensenig R, Friedman G. Magnetic nanoparticle-mediated targeting of cell therapy reduces in-stent stenosis in injured arteries. ACS Nano. 2016; 10(10):9559–69.
27. Polyak B, Fishbein I, Chorny M, Alferiev I, Williams D, Yellen B, et al. High field gradient targeting of magnetic nanoparticle-loaded endothelial cells to the surfaces of steel stents. Proc Natl Acad Sci U S A. 2008; 105(2):698–703. [PubMed: 18182491]
28. Pislaru SV, Harbuzariu A, Gulati R, Witt T, Sandhu NP, Simari RD, et al. Magnetically targeted endothelial cell localization in stented vessels. J Am Coll Cardiol. 2006; 48(9):1839–45. [PubMed: 17084259]

29. Hofmann A, Wenzel D, Becher UM, Freitag DF, Klein AM, Eberbeck D, et al. Combined targeting of lentiviral vectors and positioning of transduced cells by magnetic nanoparticles. Proc Natl Acad Sci U S A. 2009; 106(1):44–9. [PubMed: 19118196]
30. Vosen S, Rieck S, Heidsieck A, Mykhaylyk O, Zimmermann K, Bloch W, et al. Vascular repair by circumferential cell therapy using magnetic nanoparticles and tailored magnets. ACS Nano. 2016; 10(1):369–76. [PubMed: 26736067]
31. Adamo RF, Fishbein I, Zhang K, Wen J, Levy RJ, Alferiev IS, et al. Magnetically enhanced cell delivery for accelerating recovery of the endothelium in injured arteries. J Control Release. 2016; 222:169–75. [PubMed: 26704936]
32. Chorny M, Fishbein I, Yellen BB, Alferiev IS, Bakay M, Ganta S, et al. Targeting stents with local delivery of paclitaxel-loaded magnetic nanoparticles using uniform fields. Proc Natl Acad Sci USA. 2010; 107(18):8346–51. [PubMed: 20404175]
33. Chorny M, Fishbein I, Tengood JE, Adamo RF, Alferiev IS, Levy RJ. Site-specific gene delivery to stented arteries using magnetically guided zinc oleate-based nanoparticles loaded with adenoviral vectors. FASEB J. 2013; 27(6):2198–206. [PubMed: 23407712]
34. Yellen BB, Forbes ZG, Halverson DS, Fridman G, Barbee KA, Chorny M, et al. Targeted drug delivery to magnetic implants for therapeutic applications. J Magn Magn Mater. 2005; 293:647–54.
35. Kempe H, Kates SA, Kempe M. Nanomedicine's promising therapy: magnetic drug targeting. Expert Rev Med Devices. 2011; 8(3):291–4. [PubMed: 21542699]
36. Chorny M, Fishbein I, Adamo RF, Forbes SP, Folchman-Wagner Z, Alferiev IS. Magnetically targeted delivery of therapeutic agents to injured blood vessels for prevention of in-stent restenosis. Methodist DeBakey Cardiovasc J. 2012; 8(1):23–7. [PubMed: 22891107]
37. Kempe H, Kempe M, Snowball I, Wallen R, Arza CR, Gotberg M, et al. The use of magnetite nanoparticles for implant-assisted magnetic drug targeting in thrombolytic therapy. Biomaterials. 2010; 31(36):9499–510. [PubMed: 20732712]
38. Chorny M, Alferiev IS, Fishbein I, Tengood JE, Folchman-Wagner Z, Forbes SP, et al. Formulation and in vitro characterization of composite biodegradable magnetic nanoparticles for magnetically guided cell delivery. Pharm Res. 2012; 29(5):1232–41. [PubMed: 22274555]
39. O'Connor DM, O'Brien T. Nitric oxide synthase gene therapy: progress and prospects. Expert Opin Biol Ther. 2009; 9(7):867–78. [PubMed: 19463074]
40. Kong D, Melo LG, Mangi AA, Zhang L, Lopez-Ilasaca M, Perrella MA, et al. Enhanced inhibition of neointimal hyperplasia by genetically engineered endothelial progenitor cells. Circulation. 2004; 109(14):1769–75. [PubMed: 15066951]
41. Xu S, He Y, Vokurkova M, Touyz RM. Endothelial cells negatively modulate reactive oxygen species generation in vascular smooth muscle cells: role of thioredoxin. Hypertension. 2009; 54(2):427–33. [PubMed: 19564543]
42. Ignarro LJ, Buga GM, Wei LH, Bauer PM, Wu G, del Soldato P. Role of the arginine-nitric oxide pathway in the regulation of vascular smooth muscle cell proliferation. Proc Natl Acad Sci USA. 2001; 98(7):4202–8. [PubMed: 11259671]
43. Lancaster JR Jr. Simulation of the diffusion and reaction of endogenously produced nitric oxide. Proc Natl Acad Sci USA. 1994; 91(17):8137–41. [PubMed: 8058769]
44. Yong Y, Gang-Min N, Zhuo-Hui G, Xiao-Xiang Z. Modeling the diffusion of nitric oxide produced by neuronal cells in brain ischemia. Conf Proc IEEE Eng Med Biol Soc. 2005; 7:7321–4. [PubMed: 17281971]
45. Rao RS, Miano JM, Olson EN, Seidel CL. The A10 cell line: a model for neonatal, neointimal, or differentiated vascular smooth muscle cells? Cardiovasc Res. 1997; 36(1):118–26. [PubMed: 9415280]
46. Chorny M, Fishbein I, Alferiev I, Levy RJ. Magnetically responsive biodegradable nanoparticles enhance adenoviral gene transfer in cultured smooth muscle and endothelial cells. Mol Pharm. 2009; 6(5):1380–7. [PubMed: 19496618]
47. Bryan NS, Grisham MB. Methods to detect nitric oxide and its metabolites in biological samples. Free Radic Biol Med. 2007; 43(5):645–57. [PubMed: 17664129]

48. O'Brien J, Wilson I, Orton T, Pognan F. Investigation of the Alamar Blue (resazurin) fluorescent dye for the assessment of mammalian cell cytotoxicity. Eur J Biochem. 2000; 267(17):5421–6. [PubMed: 10951200]
49. Kimes BW, Brandt BL. Characterization of two putative smooth muscle cell lines from rat thoracic aorta. Exp Cell Res. 1976; 98(2):349–66. [PubMed: 943301]
50. Raines EW. PDGF and cardiovascular disease. Cytokine Growth Factor Rev. 2004; 15(4):237–54. [PubMed: 15207815]
51. Lindner V, Reidy MA. Platelet-derived growth factor ligand and receptor expression by large vessel endothelium in vivo. Am J Pathol. 1995; 146(6):1488–97. [PubMed: 7778687]
52. Galloe AM, Kelbaek H, Thuesen L, Hansen HS, Ravkilde J, Hansen PR, et al. 10-year clinical outcome after randomization to treatment by sirolimus-or paclitaxel-eluting coronary stents. J Am Coll Cardiol. 2017; 69(6):616–24. [PubMed: 28183505]
53. Tahir H, Bona-Casas C, Hoekstra AG. Modelling the effect of a functional endothelium on the development of in-stent restenosis. PLoS One. 2013; 8(6):e66138. [PubMed: 23785479]
54. Wallace CS, Champion JC, Truskey GA. Adhesion and function of human endothelial cells co-cultured on smooth muscle cells. Ann Biomed Eng. 2007; 35(3):375–86. [PubMed: 17191127]
55. Lavender MD, Pang Z, Wallace CS, Niklason LE, Truskey GA. A system for the direct co-culture of endothelium on smooth muscle cells. Biomaterials. 2005; 26(22):4642–53. [PubMed: 15722134]
56. Levitzki A. PDGF receptor kinase inhibitors for the treatment of restenosis. Cardiovasc Res. 2005; 65(3):581–6. [PubMed: 15664384]
57. Huang J, Lin SC, Nadershahi A, Watts SW, Sarkar R. Role of redox signaling and poly (adenosine diphosphate-ribose) polymerase activation in vascular smooth muscle cell growth inhibition by nitric oxide and peroxynitrite. J Vasc Surg. 2008; 47(3):599–607. [PubMed: 18295111]
58. Yun MR, Lee JY, Park HS, Heo HJ, Park JY, Bae SS, et al. Oleic acid enhances vascular smooth muscle cell proliferation via phosphatidylinositol 3-kinase/Akt signaling pathway. Pharmacol Res. 2006; 54(2):97–102. [PubMed: 16621593]
59. Fleming I, Busse R. Signal transduction of eNOS activation. Cardiovasc Res. 1999; 43(3):532–41. [PubMed: 10690325]
60. Papapetropoulos A, Garcia-Cardena G, Madri JA, Sessa WC. Nitric oxide production contributes to the angiogenic properties of vascular endothelial growth factor in human endothelial cells. J Clin Invest. 1997; 100(12):3131–9. [PubMed: 9399960]
61. Gries A, Bode C, Peter K, Herr A, Bohrer H, Motsch J, et al. Inhaled nitric oxide inhibits human platelet aggregation, P-selectin expression, and fibrinogen binding in vitro and in vivo. Circulation. 1998; 97(15):1481–7. [PubMed: 9576429]
62. Radomski MW, Palmer RM, Moncada S. Endogenous nitric oxide inhibits human platelet adhesion to vascular endothelium. Lancet. 1987; 2(8567):1057–8. [PubMed: 2889967]
63. Kubes P, Suzuki M, Granger DN. Nitric oxide: an endogenous modulator of leukocyte adhesion. Proc Natl Acad Sci USA. 1991; 88(11):4651–5. [PubMed: 1675786]
64. Pfeiffer T, Wallich M, Sandmann W, Schrader J, Godecke A. Lipoplex gene transfer of inducible nitric oxide synthase inhibits the reactive intimal hyperplasia after expanded polytetrafluoroethylene bypass grafting. J Vasc Surg. 2006; 43(5):1021–7. [PubMed: 16678699]
65. Wang Y, Lam KS, Xu JY, Lu G, Xu LY, Cooper GJ, et al. Adiponectin inhibits cell proliferation by interacting with several growth factors in an oligomerization-dependent manner. J Biol Chem. 2005; 280(18):18341–7. [PubMed: 15734737]
66. Arita Y, Kihara S, Ouchi N, Maeda K, Kuriyama H, Okamoto Y, et al. Adipocyte-derived plasma protein adiponectin acts as a platelet-derived growth factor-BB-binding protein and regulates growth factor-induced common postreceptor signal in vascular smooth muscle cell. Circulation. 2002; 105(24):2893–8. [PubMed: 12070119]

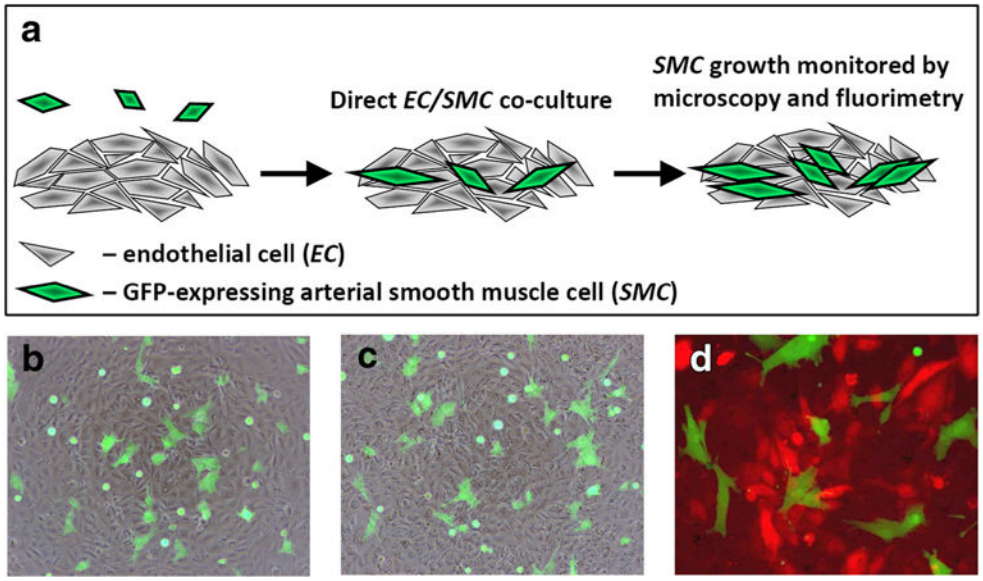

Fig. 1.

Direct contact co-culture assay for selectively monitoring growth of proliferative vascular SMC in the presence of functionalized EC (schematically shown in **a**). Stably GFP-expressing SMC reproducing key features of neointimal cells (A10 cell line) are seeded on top of an EC monolayer. Their morphology and expansion are then monitored continuously by fluorescent microscopy using the standard fluorescein wavelength settings. SMC proliferation over time is quantitatively measured by fluorimetry ($\lambda_{ex}/\lambda_{em}$ = 485 nm/535 nm). Merged (green/bright field channels) images show GFP-expressing A10 several hours post seeding on confluent bovine aortic endothelial cells (BAEC) without or with prior BAEC treatment with zinc oleate-based MNP (**b** and **c**, respectively). A merged (green/red channels) image in **d** shows distinct and cell type-specific fluorescence patterns of GFP-expressing A10 in direct contact co-culture with BAEC pretreated magnetically with MNP impregnated with Ad encoding the red fluorescent protein (RFP) as a model transgene. Original magnification is ×40

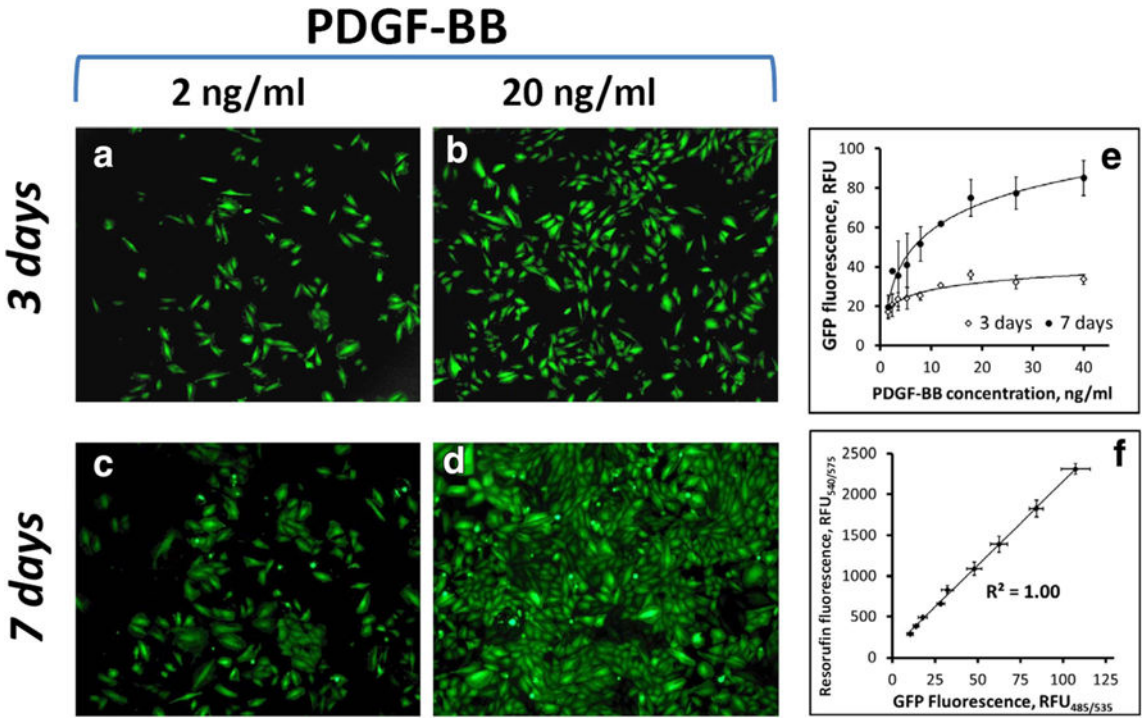

Fig. 2.

Response to stimulation with PDGF-BB and fluorescence-based quantification of cultured GFP-expressing A10 cells. Proliferative SMC derived from the thoracic aorta of embryonic rats and lentivirally induced to stably express the GFP reporter ($_{GFP}$A10) exhibit PDGF-BB dose-dependent expansion as shown by fluorescent microscopy at days 3 (**a**, **b**) and 7 (**c**, **d**) post seeding. $_{GFP}$A10 expansion as a function of PDGF-BB concentration quantified fluorimetrically shows a saturation pattern, with cell proliferation rates reaching their maximal levels at 20 ng/ml of the mitogen (**e**). Original magnification is ×40. The results of the GFP fluorescence-based assay show strong correlation with those obtained using another well-established method (Alamar Blue assay), where the number of viable cells is quantified based on their metabolic activity causing reduction of resazurin into a strongly red fluorescent dye, resorufin (**f**). Data in **e** and **f** are presented as mean ± SD

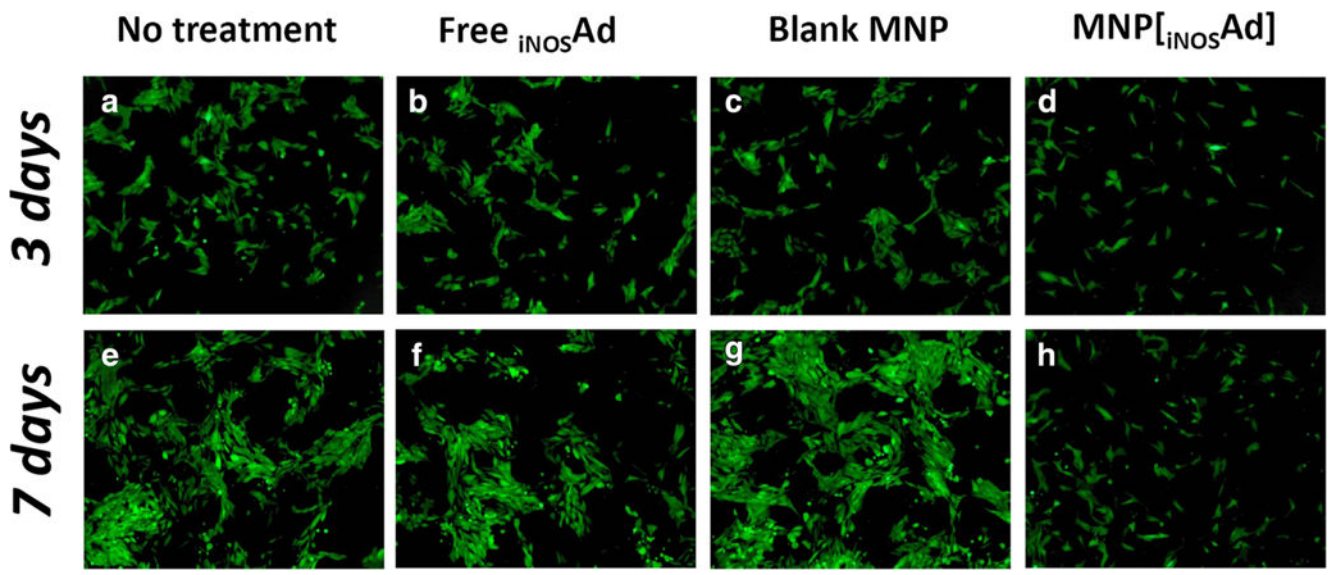

Fig. 3.

The effect of BAEC functionalization with inducible NO synthase (iNOS) on expansion of co-cultured $_{GFP}$A10. BAEC were either left untreated (**a**, **e**), or treated with free $_{iNOS}$Ad (**b**, **f**), Ad-free (blank) MNP (**c**, **g**) or MNP[$_{iNOS}$Ad] (**d**, **h**). Co-cultured green fluorescent $_{GFP}$A10 were microphotographed using the standard fluorescein wavelength settings on day 3 and day 7 (*upper* and *lower panels*, respectively). Original magnification is ×40

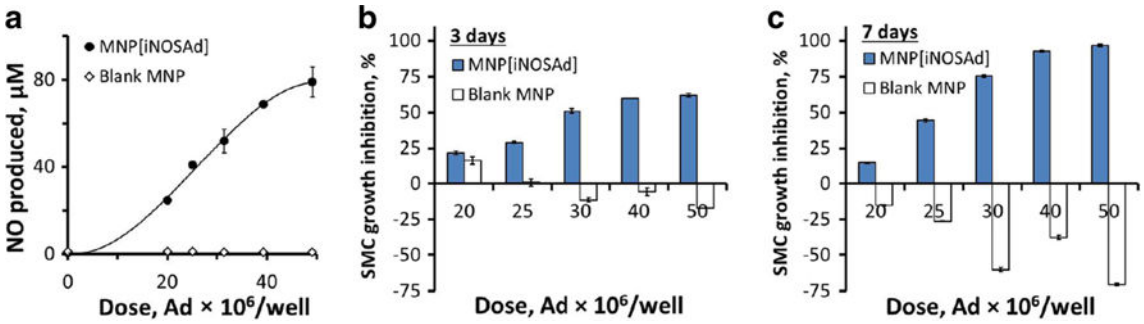

Fig. 4.

Magnetically facilitated functionalization of EC with MNP[$_{iNOS}$Ad], and its effect on NO synthesis and expansion of co-cultured $_{GFP}$A10, in comparison to equivalent doses of Ad-free (blank) MNP. EC-associated NO synthesis was determined on day 3 by the Griess assay (**a**). The effect of BAEC pretreatment on $_{GFP}$A10 expansion was quantified fluorimetrically based on GFP fluorescence and expressed as % cell growth inhibition after 3 and 7 days (**b** and **c**, respectively). Data are presented as mean ± SD

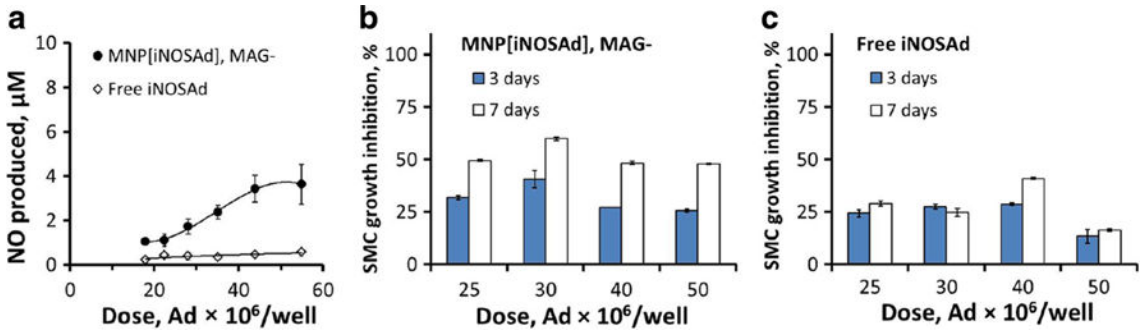

Fig. 5.

The effect of non-magnetic pretreatment of BAEC with MNP[$_{iNOS}$Ad] or free $_{iNOS}$Ad on NO synthesis (**a**, 3 days) and proliferation of co-cultured $_{GFP}$A10 cells (**b** and **c**, respectively). Data are presented as mean ± SD

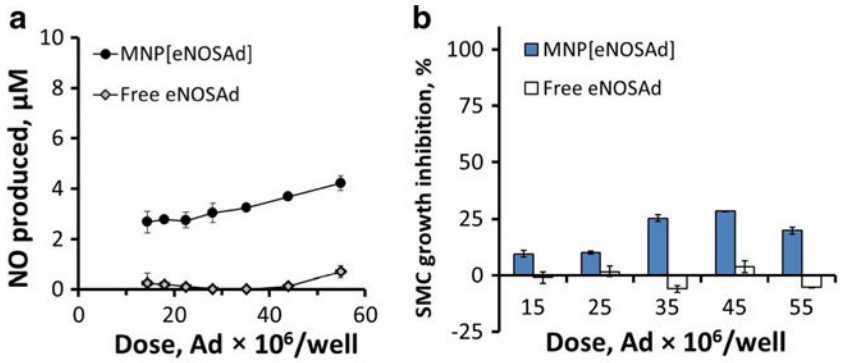

Fig. 6.

The effect of magnetically driven BAEC transduction with the endothelial isoform of NO synthase (eNOS) using MNP[$_{eNOS}$Ad] vs. free $_{eNOS}$Ad on NO synthesis (**a**, 3 days) and proliferation of co-cultured $_{GFP}$A10 cell (**b**, 7 days). Data are presented as mean ± SD